

AN OXIDATION-RESISITANT MEASUREMENT APPARATUS

Dong-Yang An, Jing-Min Dai, Peng Xiao

Harbin Institute of Technology, School of Electrical Engineering and Automation, Harbin 150001,
People's Republic of China (ady@hit.edu.cn, djm@hit.edu.cn, +86 0451 8641 5146, xp_hit@126.com)

Abstract

On the basis of induction heating, radiation heating and liquid nitrogen refrigeration, high-temperature, medium-temperature, normal-temperature and low-temperature heating/refrigeration furnaces were designed, respectively. An apparatus with a wide temperature range and high accuracy applied to test oxidation resistance of materials has been developed based on the thermogravimetric method and the heat transfer principle. The apparatus consists of four heating/cooling systems, a specimen fixture positioning unit, a laser positioning unit, vertical and horizontal moving guide rails, and a high-precision weighing balance. The apparatus, based on the thermogravimetric method, is able to test oxidation resistance of materials. In the test, the temperature range was $-180\sim 3000^{\circ}\text{C}$ (the highest temperature is determined by material properties). The temperature control accuracy was $\pm 5^{\circ}\text{C}$. The accuracy of on-line weighing was ± 0.1 mg. The measurement uncertainty was 0.2 mg. Compared with other relevant devices, this apparatus has its own advantages: simple operation, wide heating/cooling temperature range, sufficient specimen heating, high sensitivity and precision, and short heating/cooling time. The experimental results show that the developed apparatus presented in this study not only can be used for isothermal thermogravimetric tests, but also for thermal cycling tests and multi-step oxidation tests. With the effective integration of multiple heating apparatus and refrigeration apparatus, the apparatus breaks through the limitations of the heating/cooling temperature range of the existing devices, accomplishes the high-precision oxidation resistance test of materials in a wide temperature range, and will play a great role in improving the research of materials.

Keywords: coating, apparatus, oxidation resistance, wide temperature range, high precision.

© 2019 Polish Academy of Sciences. All rights reserved

1. Introduction

With the extending research and application, the oxidation resistance of materials has become one of important factors limiting their applications, especially those working in high-temperature conditions [1–3]. Thermogravimetric analysis is an important method to measure the oxidation resistance of materials [4, 5]. Thermal performance data obtained by thermogravimetric analysis is an important basis to measure whether the material can satisfy the needs of thermal process.

In order to improve the research on thermogravimetric technique, scholars and research institutes in related fields from China, the United States, Russia, France, Germany, Netherlands,

Norway, India, Japan, and Serbia have made great efforts in the research on various specimen specifications and purposes [6–19]. Most of the studies are intended to increase temperature range, specimen weight range, heating rate, temperature accuracy, and weighing accuracy of thermogravimetric systems. Representative thermogravimetric devices are TA's Q600 thermo-gravimeter and Netzsch's STA449F3 series. Their temperature ranges are 20~1500°C and –150~2400°C, respectively [20, 21]. However, there are still some limitations in these devices, such as too small temperature range, insufficient specimen heating and fragility.

Based on the thermogravimetric method and the heat transfer principle, a high-precision oxidation resistance testing apparatus in a wide temperature range is designed. The hanging method is adopted to heat and weigh specimens. This apparatus has its own advantages, for instance, simple operation, wide heating/cooling temperature range, sufficient specimen heating, high sensitivity and precision, and short heating/cooling time. To verify the effectiveness of the testing apparatus, a Niobium-Hafnium substrate coated with silicide has been tested by this apparatus.

2. High-temperature heating and low-temperature refrigeration

2.1. High-temperature heating

At present, ultra-high-temperature (above 2000°C) heating methods in the air mainly include the high-power laser heating method, optical radiation heating method, induction heating method and direct electric heating method, which are shown in Table 1.

Table 1. High-temperature heating methods.

Heating mode	Heating body	Temperature range
high-power laser heating	Heat conductor	Room temperature ~5000°
optical radiation heating	The specimen body	Room temperature ~2600°
induction heating	The specimen body	Room temperature ~3000°
direct electric heating	Brass (cooling protection), graphite, <i>etc.</i>	Room temperature ~3000°

The advantages of high-power laser heating method are: direct heating, fast heating and easy control. However, it is expensive and fragile. The optical radiation heating with simple furnace structure can also directly radiate a specimen. However, it is difficult to cumulate energy and accomplish the ultra-high-temperature heating. Induction heating can directly heat a specimen without considering the heat resistance of the heating body, but it has low efficiency of heating flat specimens in a tube-type induction coil. The direct electric heating is relatively inexpensive, easy to control and mature in technology. However, it is difficult to protect the heating body in severe temperature and atmospheric conditions.

2.2. Low-temperature refrigeration

Ultra-low-temperature refrigeration is a mature technology at present. Ultra-low-temperature refrigeration methods mainly include liquid nitrogen refrigeration and refrigerator cooling. They are shown in Table 2.

The advantages of refrigerator are its simple operation and no need of using liquid gas. However, it requires circulating water to cool the compressor and a vacuum pump to achieve

Table 2. Ultra-low-temperature refrigeration methods.

Refrigeration mode	Temperature range
refrigerator cooling	Room temperature ~ -180° determined by model
liquid nitrogen refrigeration	Room temperature ~ -180°

vacuum in the specimen chamber. The advantages of liquid nitrogen refrigeration include: simple structure, convenient operation, low price, short refrigeration time and no additional dry air. Nevertheless, a disadvantage is that the specimen chamber is easily subjected to frosting.

3. Heating principle and heating model

In this study, in the method of high-temperature heating the specimen is placed in the induction heating system. The induction heating system causes eddy current in the specimen which results in forming an alternating magnetic field, and finally converts electric energy into heat energy to heat the specimen. The specimen temperature is adjusted by changing the input power (W_1).

The efficiency of induction heating is expressed as follows:

$$\eta = \frac{1}{1 + \frac{d_1}{d_2} \sqrt{\frac{\rho_1}{\mu_2 \rho_2}}}, \quad (1)$$

where: d_1 and d_2 are diameters (m) of the induction heating coil and the specimen, respectively; ρ_1 and ρ_2 are resistivity ($\Omega \cdot \text{m}$) of the induction coil and the specimen, respectively; μ_2 is the relative permeability of specimen. According to the law of conservation of energy, the input power of induction heating is equal to the sum of effective power P_1 , radiant heat loss P_2 and convective heat loss P_3 [22]. Accordingly:

$$\eta W_1 = P_1 + P_2 + P_3. \quad (2)$$

The following is based on formula:

$$W_1 \frac{1}{1 + \frac{d_1}{d_2} \sqrt{\frac{\rho_1}{\mu_2 \rho_2}}} = \frac{CG(t_2 - t_1)}{t} + \sigma \varepsilon \left[\left(\frac{T_2}{100} \right)^4 - \left(\frac{T_1}{100} \right)^4 \right] S + \pi d H h \Delta t. \quad (3)$$

In the formula above, C is the specific heat capacity ($\text{kJ/kg} \cdot ^\circ\text{C}$) of the specimen, is the mass of specimen (kg), G is the temperature ($^\circ\text{C}$) before heating and is the target temperature ($^\circ\text{C}$). σ is the blackbody radiation constant. T_1 is the air thermodynamic temperature ($^\circ\text{C}$). T_2 is the thermodynamic temperature ($^\circ\text{C}$) of the surface of the specimen after heating. ε is the surface emissivity of the specimen. S is the effective heat dissipation area (m^2). d is the bottom diameter and H is the height of the furnace body, respectively. h is the convective heat transfer coefficient. is the temperature gradient.

When heated at medium and room temperatures, the specimen is placed in an isothermal chamber, in which temperature is controlled by adjusting the input power W_2 , and the specimen is heated by radiation. The heating model is expressed as follows:

$$W_2 = \frac{CG(t_2 - t_1)}{t} + \sigma \varepsilon \left[\left(\frac{T_2}{100} \right)^4 - \left(\frac{T_1}{100} \right)^4 \right] S + \pi d H h \Delta t. \quad (4)$$

4. Apparatus description

4.1. Testing platform

Based on the thermogravimetric analysis method and the heat transfer principle, an apparatus for oxidation resistance test over a wide temperature range ($-180\sim 3000^{\circ}\text{C}$) has been developed. Its structure is shown in Fig. 1. The apparatus mainly consists of four heating/refrigeration furnaces (high-temperature furnace, moderate temperature furnace, normal-temperature furnace, and low-temperature furnace), a specimen moving system (consisting of vertical and horizontal moving rails, a specimen fixture positioning device, and a laser locator), and a high-precision weighing balance. Specimens are hung in different furnaces for heating or cooling (clamped by high-temperature oxidation-resistant chucks or suspended by platinum wires).

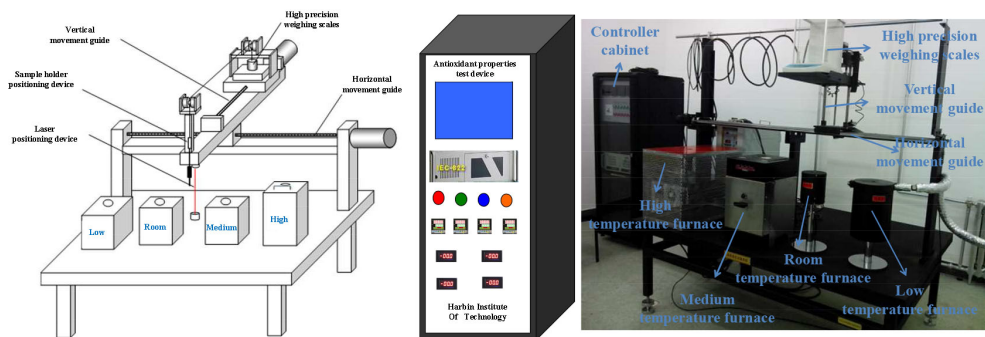


Fig. 1. An overview of test apparatus.

On the workbench, support parts of the specimen moving system are installed in parallel to four heating/refrigeration furnaces. The horizontal moving rail drives the specimen fixture positioning apparatus and the high-precision weighing balance to move horizontally in the direction parallel to four furnaces, which makes specimens move along different furnaces. The vertical moving rail drives the specimen weighing balance to drag the specimen fixture positioning apparatus up and down in the direction perpendicular to the furnace. Thus, the specimen can be lifted into and out of different furnaces. The specimen moving system is positioned by the laser locator. The laser locating emitter is vertically mounted beneath the specimen moving arm, while the laser locating receiver is mounted near the heating furnace. Once the receiver receives a signal from the emitter, the specimen movement will be stopped.

4.2. High-temperature heating furnace

A high-temperature heating furnace heats specimens by induction heating and convection heat transfer. The high-temperature heating furnace designed in this research is shown in Fig. 2. Induction coils uniformly wrap external surface of high-temperature-resistant cylindrical ceramic. Specimens clamped by high-temperature oxidation-resistant chucks or suspended by platinum wires are heated in the furnace. An alternating magnetic field is generated by induction, causing eddy currents inside the specimen to heat the specimen.

In a high-temperature furnace, specimen temperature was measured with a fibre-optic pyrometer at a heating frequency of 30~100 kHz. The heating temperature range is $1400\sim 3000^{\circ}\text{C}$. The temperature control accuracy is $\pm 5^{\circ}\text{C}$ and the temperature measurement accuracy is $\pm 1^{\circ}\text{C}$.

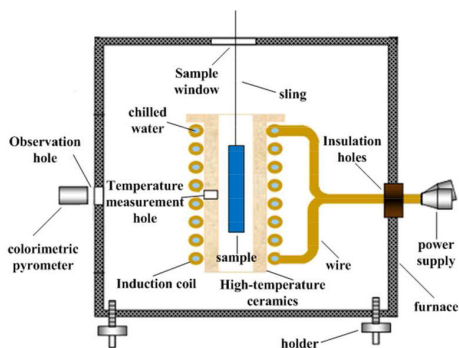


Fig. 2. A schematic diagram of the high-temperature chamber.

The induction coils are cooled by water. The high-temperature-resistant ceramic is used to support induction coils and to produce an isothermal zone when the specimen is heated. A round hole right at the top of the high-temperature-resistant ceramic tube enables moving and on-line weighing of the specimen; through this hole the specimen is put into the central region of the high-temperature-resistant ceramic tube for induction heating. Another circular hole placed in the middle of the high-temperature-resistant ceramic tube enables the fibre-optic pyrometer to measure temperature of the specimen in real time.

4.3. Moderate-temperature chamber

A moderate-temperature furnace heats specimens by radiative heat transfer and convection heat transfer. It also uses a helical graphite electrode to heat specimens. Inside the electrode, a corundum tube serves as the heat-resistant body so that its inner surface forms an effective isothermal heating zone, which guarantees that a specimen is heated uniformly in the heating zone. Insulation and thermal insulation materials are used by the external heating electrode.

Contact temperature measurement of a specimen in a moderate-temperature furnace is performed with a type-B thermocouple. The temperature range is 100~1500°C. The temperature control accuracy is $\pm 5^\circ\text{C}$ and the temperature measurement accuracy is $\pm 1^\circ\text{C}$. From the middle isothermal zone in the internal surface of the corundum tube to the furnace surface, an optical window is opened to monitor temperature inside the furnace and temperature of the specimen.

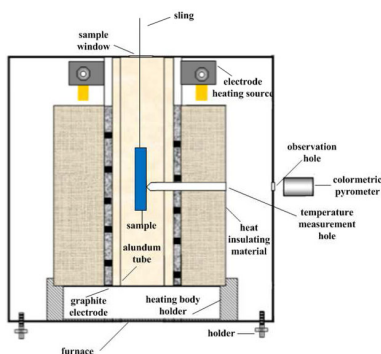


Fig. 3. A schematic diagram of the moderate-temperature chamber.

4.4. Normal-temperature furnace

A normal-temperature furnace heats specimens by radiative heat transfer and convective heat transfer. It uses resistor films to heat specimens. An aluminium tube is used as the heat-resistant body inside the electrode so that its inner surface forms an effective isothermal heating zone, which guarantees that a specimen is heated uniformly in the heating zone. The heating film is surrounded with thermal barrier insulation material for thermal insulation.

Contact temperature measurement of a specimen in a normal-temperature furnace is performed with a PT100 platinum resistor. The temperature ranges from room temperature to 120°C. The temperature control accuracy is $\pm 1^\circ\text{C}$ and the temperature measuring accuracy is $\pm 0.5^\circ\text{C}$. From the middle isothermal zone in the internal surface of the aluminium tube to furnace surface, an optical window is opened to monitor temperature inside the furnace and temperature of the specimen.

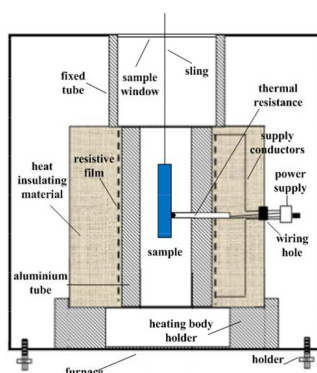


Fig. 4. A schematic diagram of the normal-temperature chamber.

4.5. Low-temperature refrigeration furnace

Specimens in a low-temperature refrigeration furnace are cooled by means of liquid nitrogen refrigeration and heated by the resistance wire heating method. A thermally conductive chamber is put into a Dewar container. Outside the chamber, liquid nitrogen is filled to refrigerate the specimen, which enables formation of an effective isothermal refrigeration zone within the chamber. The middle of the specimen chamber is uniformly wound by resistance wires for ohmic heating, resulting in an effective isothermal heating zone inside the chamber. With a combination of the above two methods, the heating and cooling of specimens can be achieved.

For specimens in a low-temperature refrigeration/heating furnace, contact temperature measurement is performed with a PT100 platinum resistor. To ensure closure of the specimen chamber, temperature of the specimen is obtained by measuring temperature of the effective isothermal zone in the chamber. The refrigeration temperature ranges from -180°C to room temperature. The temperature control accuracy is $\pm 1^\circ\text{C}$. The temperature measurement accuracy is $\pm 0.5^\circ\text{C}$. A round hole at the top of the furnace enables moving and real-time weighing of the specimen. In the upper portion of the specimen chamber, another hole situated near the outlet enables nitrogen to enter the specimen chamber to generate positive pressure air. In this way, water vapour is prevented from entering the specimen chamber, thus avoiding its freezing or frosting.

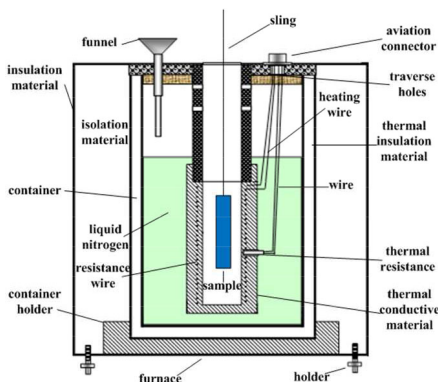


Fig. 5. A schematic diagram of the low-temperature chamber.

4.6. Platinum wires and high-temperature oxidation-resistant chucks

Hanging a specimen on a platinum wire or holding it by a high-temperature oxidation-resistant chuck is chosen on the basis of the specimen's size and shape. The high-temperature oxidation-resistant chuck is made of a new ceramic material and consists of two pieces of high-temperature ceramics. Its top is fixed with stainless steel screws for holding and removing the specimen, so that the chuck can be used in oxidative atmosphere at 2000°C or above for a long time. The chuck is lifted by a stainless steel sling and connected with the specimen moving mechanism. The length of the chuck is 70~80 mm, which ensures a sufficient heat diffusion distance. The structure diagram and photo of the oxidation-resistant chuck are shown in Fig. 6. The high-temperature chuck is made of a new type of ceramic material, developed and produced by Shandong Qingkong Qingtian High-Tech Products Co., Ltd. The main technical parameters of the material are shown in Table 3.

Table 3. Main parameters of the high-temperature chuck material.

Melting Point	3200°
Resistivity	100–2000 $\mu\Omega \cdot \text{cm}$
Density	4.8–6 $\text{g} \cdot \text{cm}^{-3}$
Densification	96%
Bending Strength	3.3×10^{-4} MPa
Rockwell Hardness	92
Ablation Rate or Oxidation Resistance	Oxygen-acetylene flame 1950°, 3.2×10^{-5} mm/s
Thermal Expansion Coefficient	25–1500, $7.2 \times 10^{-6}/\text{DEG}$
Thermal Conductivity	25.2 kcal/(m·h·°C)
Vapour Pressure	4.3×10^{-3} (1800°)
Thermal Shock Resistance	No burst occurs when being put into water at 1200° repeatedly for 5 times
Production Method	Hot Pressed Sintering at 2100° under 200 MP Isostatic Pressure

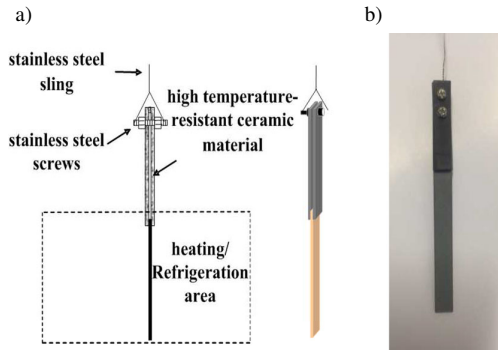


Fig. 6. A schematic of the high-temperature oxidation-resistant chuck. a) Structure; b) actual object.

4.7. Control system

The control system of the oxidation resistance test apparatus consists of an industrial control computer, a temperature regulating meter, a digital temperature display, and a power output component. It can accomplish the on-line temperature data collection and control of the furnace and specimen, control of specimen movement, specimen quality change as well as the signal collection and recording of images. A block diagram of the control system is shown in Fig. 7.

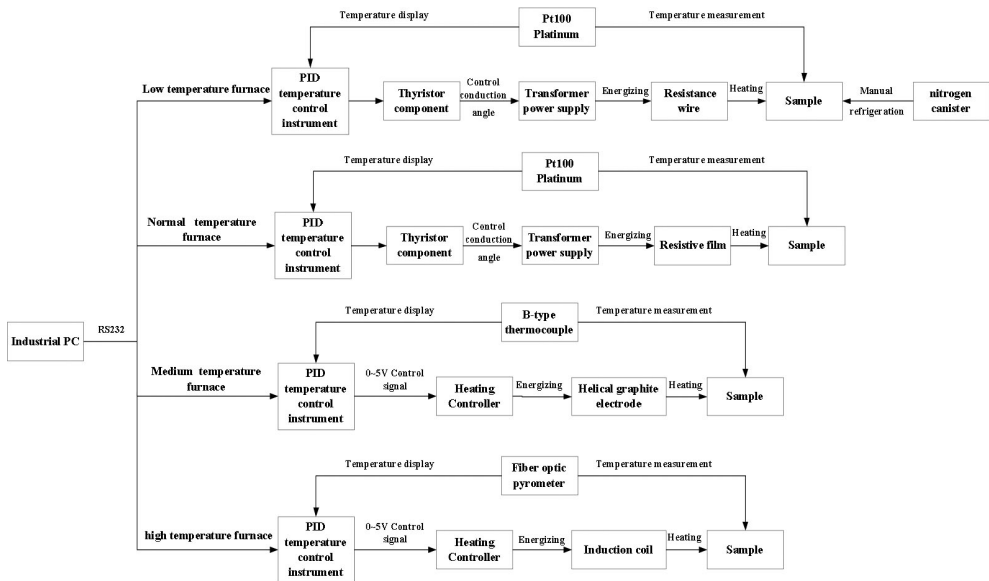


Fig. 7. Control system.

During the test, furnace temperature, specimen temperature and video signal of specimen are all transmitted to a control cabinet for display, storage, analysis and calculation. The control cabinet sends the control signal to the temperature control apparatus of each furnace and specimen transmission parts through cables. The test can be controlled manually or fully automatically. The software interface is shown in Fig. 8.

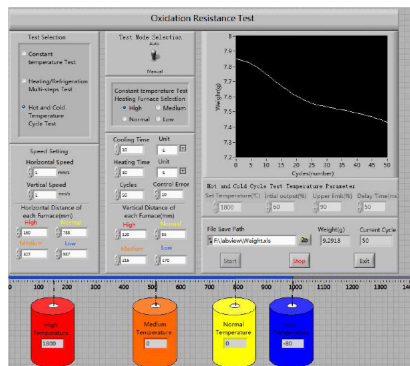


Fig. 8. Software interface.

5. Results and uncertainty analysis

In this study, a Niobium–Hafnium substrate coated with silicide (Si–Cr–Ti) is selected to carry out relevant experiments to verify the effectiveness of the apparatus. The length, width and thickness of the substrate are 70×10^{-3} m, 10×10^{-3} m and 1×10^{-3} m, respectively.

1. Isothermal thermogravimetric test: According to the actual working temperature of the material, the test temperature of the corresponding furnace body can be set. The test temperatures of the four heating furnaces (the high-temperature one, the medium-temperature one, the room-temperature one and the low-temperature heating/refrigeration one) are set to 1800°C , 1400°C , 100°C , and -80°C , respectively. The specimen weight is obtained with the on-line weighing method. The total test time of each furnace body is 5 hours. The weighing interval is 1 hour. The experimental results are shown in Figs. 9a–9d.
2. Multi-step oxidation test: the test temperatures are set to -80°C , 100°C , 1400°C and 1800°C at low-, room-, medium- and high-temperature heating, respectively. The total test time is 4 hours. The heating/ refrigeration time of a single furnace body is 1 hour. Each specimen is weighed on-line after taking it out from the furnace and cooling/heating to room temperature. The weighing interval is 1 hour. The test results are shown in Fig. 9e.
3. Thermal cycling test: the low-temperature heating/refrigerating furnace and the high-temperature furnace are selected to carry out the thermal cycling test. The test temperature of the high-temperature furnace is 1800°C , the low-temperature refrigeration temperature is -80°C , the total number of thermal cycling tests is 50, and the heating time and refrigeration time are both 10 seconds. The specimen weight is obtained with the on-line weighing method after a single thermal cycling test. The test results are shown in Fig. 9f.

As shown in Figs. 9a–9d, the specimen weight increases firstly and then decreases in the heating environment, and increases continuously in the refrigerating environment. We deduced primarily that the increasing of the specimen weight at the beginning of heating is caused by the chemical reaction between the specimen and oxygen. When the oxidation accumulates to a certain level, the oxidation products will fall off due to the effect of surface thermal stress, and the specimen mass becomes smaller. For the low-temperature test, the specimen weight keeps increasing all the time. Moreover, the longer the refrigerating time, the slower the increase of the specimen weight. The reason lies in the frosting on the surface of the specimen, which results in the weight increase. After refrigeration for a period of time, the decreased surface viscosity of the material leads to slight shedding, thus, the weight increase of the specimen slows down.

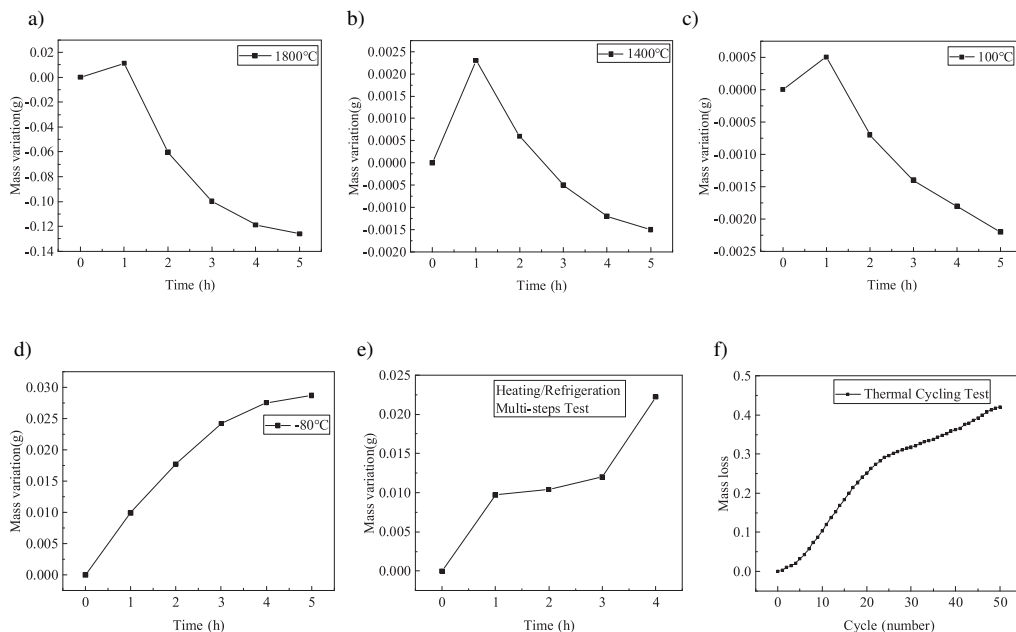


Fig. 9. Relationship between mass variation of a specimen and test time or number of thermal cycling tests: a) high-temperature test; b) moderate-temperature test; c) normal-temperature test; d) low-temperature test; e) multi-step oxidation test; f) thermal cycling test.

As shown in Fig. 9e, in the multi-step oxidation test, the increase of the specimen weight is rapid at first, then slows down, and finally shows the rapid trend again. It can be explained as follows: In the low-temperature test, the increase of the specimen weight is probably caused by frost on its surface, since the weight of the specimen has been obtained at room temperature. In the room-temperature test, it is due to the oxidation of the surface. However, in the medium-temperature test, the increase shows a slowing trend since the oxidation has accumulated to a certain extent. Finally, in the high-temperature test, the increase becomes rapid again because of the fast oxidation caused by a relatively high testing temperature. As shown in Fig. 9f, in the thermal cycling test, the specimen mass shows a constant decreasing trend which may be due to the oxidation reaction of the specimen in the high-temperature heating test and the spallation of its surface in the low-temperature refrigeration. Due to the rapid and drastic change of temperature, the specimen weight decreases gradually. The results of this study are basically consistent with those obtained in Institute for Advanced Ceramics, Harbin Institute of Technology and Materials Architecturing Research Center, Korea Institute of Science and Technology [23, 24].

In this research, uncertainty mainly stems from weighing balance uncertainty and environment factors. The factors of weighing balance uncertainty consist of differences in measurements of the same load in multiple runs, deviation of indicated value at each load point from mass of standard weights, indication error of a load at difference positions, the maximum permissible error or expanded uncertainty of standard weights, the minimum effectively distinguishable indication error, and capability of responding to a tiny load. Environmental factors consist of temperature, humidity, atmospheric pressure, air buoyance, gravity acceleration, electromagnetic field, air flow, and vibration. Dominant factors are repeated measurement with the weighing balance, the maximum permissible error, standard weight errors of the weighing balance and indication errors

caused by temperature instability and vibration [25, 26]. The result of the uncertainty analysis is shown in Table 4.

Table 4. Uncertainty budget.

Uncertainty component	Symbol and calculation	Standard uncertainty /mg
repeated measurement	$u(m_1)$	0.07
the maximum permissible error	$u(m_2)$	0.17
standard weights error (F1)	$u(m_3)$	0.05
temperature instability and vibration	$u(m_4)$	0.06
Combined uncertainty	$u = \sqrt{u^2(m_1) + u^2(m_2) + u^2(m_3) + u^2(m_4)}$	0.20
Expanded uncertainty ($k = 2$)	$u(m_1)$	0.40

6. Conclusion

In the oxidation resistance test apparatus, temperature ranges from -180°C to 3000°C (The maximum heating temperature depends on the material itself) in heating/cooling environment. The temperature control accuracy is $\pm 5^{\circ}\text{C}$. The on-line weighing accuracy is ± 0.1 mg and standard measurement uncertainty is 0.2 mg (coverage factor = 2). Compared with other relevant devices, this apparatus has its own advantages: simple operation, wide heating/cooling temperature range, sufficient specimen heating, high sensitivity and precision, as well as short heating/cooling time. The experimental results show that the apparatus presented in this study not only can carry out thermogravimetric tests of materials in isothermal conditions, but also thermal cycling tests and multi-step oxidation tests. Through the effective integration of multiple heating and refrigeration apparatus, it breaks through the limitations of the existing devices regarding heating/refrigerating temperature range, it is capable to perform the high-precision oxidation resistance test of materials in a wide temperature range, and will greatly boost the research of materials.

Acknowledgments

This paper is supported by National Defense Technical Basic Research Program of China (Grant No. JSZL2015603B002) and Aviation Science Fund Project (Grant No. 20172777007).

References

- [1] Perepezko, J.H., Sakidja, R. (2010). Oxidation-resistant coatings for ultra-high-temperature refractory mo-based alloys. *Adv. Eng. Mater.*, 11(11), 892–897.
- [2] Koo, C.H., Yu, T.H. (2000). Pack cementation coatings on ti 3 al–nb alloys to modify the high-temperature oxidation properties. *Surf. Coat. Technol.*, 126(2), 171–180.
- [3] Beresnev, A.G., Logachev, A.V., Razumovskii, I.M. (2012). Theoretical analysis of the alloying system and principles of the creating of a new generation of high-temperature nickel alloys by method of the granular metallurgy. *Genome. Res.*, 12(1), 3–15.

- [4] Kastanaki, E., Vamvuka, D., Grammelis, P. (2002). Thermogravimetric studies of the behavior of lignite-biomass blends during devolatilization. *Fuel. Process. Technol.*, 77(02), 159–166.
- [5] Horowitz, H.H., Metzger, G. (1999). A New Analysis of Thermogravimetric Traces. *Astron. Astrophys.*, 353(1), 177–185.
- [6] Xiong, Y., Jiang, T., Zou, X. (2003). Automatic proximate analyzer of coal based on isothermal thermogravimetric analysis (tga) with twin-furnace. *Thermochim. Acta.*, 408(1), 97–101.
- [7] Sarwar, A., Khan, M.N., Azhar, K.F. (2012). Kinetic studies of pyrolysis and combustion of thar coal by thermogravimetry and chemometric data analysis. *J. Therm. Anal. Calorim.*, 109(1), 97–103.
- [8] Meng, A., Chen, S., Long, Y., Zhou, H., Zhang, Y., Li, Q. (2015). Pyrolysis and gasification of typical components in wastes with macro-tga. *Waste. Manage.*, 157(3), 1–8.
- [9] Gracik, T.D., Long, G.L., Sorathia, U.A.K., Douglas, H.E. (1992). A novel thermogravimetric technique for determining flammability characteristics of polymeric materials. *Thermochim. Acta.*, 212(2), 209–217.
- [10] Kettrup, A., Matuschek, G., Utschick, H., Namendorf, C., Bräuer, G. (1997). A macro sta-system for environmental samples. *Thermochim. Acta.*, 295(1–2), 119–131.
- [11] Mikkelsen, L., Solvang, M., Larsen, P.H., Blumm, J. (2005). Novel instrument for high temperature thermogravimetric measurements in high water vapour contents. *J. Therm. Anal. Calorim.*, 80(3), 775–780.
- [12] Mennoud, F., Golfier, F., Salvador, S., Van, D.S.L., Dirion, J.L. (2018). Experimental and numerical study of steam gasification of a single charcoal particle. *Combust. Flame.*, 145(1), 59–79.
- [13] L'Vov, B.V. (2009). Role of vapour oversaturation in the thermal decomposition of solids. *J. Therm. Anal. Calorim.*, 96(1), 321–330.
- [14] Becidan, M., Skreiberg, Ø., Hustad, J.E. (2007). Products distribution and gas release in pyrolysis of thermally thick biomass residues samples. *J. Anal. Appl. Pyrolysis.*, 78(1), 207–213.
- [15] Devaraju, J.T., Suresha, P.H., Ramani, Radhakrishna, M.C. (2011). Development of microcontroller based thermogravimetric analyzer. *Measurement.*, 44(10), 2096–2103.
- [16] Chen, W.H., Pochih, K. (2011). Torrefaction and co-torrefaction characterization of hemicellulose, cellulose and lignin as well as torrefaction of some basic constituents in biomass. *Energy*, 36(2), 803–811.
- [17] Ma, S., Huang, G., Hill, J.O. (1991). Knis – a computer program for the systematic kinetic analysis of non-isothermal thermogravimetric data. *Thermochim. Acta*, 184(2), 233–241.
- [18] Cardinale, G.F., Howitt, D.G., Mccarty, K.F., Medlin, D.L., Mirkarimi, P.B., Moody, N.R. (1996). Analysis of residual stress in cubic boron nitride thin films using micromachined cantilever beams. *Diam. Relat.*, 5(11), 1295–1302.
- [19] Long, Y., Meng, A., Shen, C., Hui, Z., Zhang, Y., Li, Q. (2017). Pyrolysis and combustion of typical wastes in a newly designed macro-tga: characteristics and simulation by model components. *Energ. Fuel.*, 31(7), 7582–7590.
- [20] Westrich, T.A., Dahlberg, K.A., Kaviany, M., Schwank, J.W. (2011). High-temperature photocatalytic ethylene oxidation over TiO₂. *J. Phys. Chem. C.*, 115(33), 16537–16543.
- [21] Wang, Y.T., Lu, A.H., Li, W.C. (2012). Mesoporous manganese dioxide prepared under acidic conditions as high performance electrode material for hybrid supercapacitors. *Microporous Mesoporous Mat.*, 153(6), 247–253.
- [22] An, D.Y., Dai, J.M., Xiao, P. (2019). Modelling the heat transfer of an antioxidant coating heating system in wide temperature and simulation. *Results. Phys.*, 12,124–131.

- [23] Ge, Y., Wang, Y., Chen, J. (2018). An Nb₂O₅-SiO₂-Al₂O₃/NbSi₂/Nb₅Si₃, multilayer coating on Nb-Hf alloy to improve oxidation resistance. *J. Alloy. Compd.*, 745, 271–281.
- [24] Choi, Y.J., Yoon, J.K., Kim, G.H., Yoon. (2017). High temperature isothermal oxidation behavior of nbsi2 coating at 1000 – 1450°C. *Corros. Sci.*, 129, S0010938X1730330X.
- [25] González, A.G., Herrador, M.Á. (2007). The assessment of electronic balances for accuracy of mass measurements in the analytical laboratory. *Accredit. Qual. Assur.*, 12(1), 21–29.
- [26] Reichmuth, A., Wunderli, S., Weber, M. (2004). The uncertainty of weighing data obtained with electronic analytical balances. *Microchim. Acta.*, 148(3–4), 133–141.